Seismic displacement response of surface footings in sand

Raj Siddharthan & Gary Norris
University of Nevada-Reno, USA

ABSTRACT: A method of analysis that accounts for degradation of soil properties to evaluate seismic displacments of footings is described. Predicted footing response compares well with the available laboratory data. Investigations reveal that the influence of the rocking of the structure, the location of the water table, and contact pressure are important factors that govern settlement response. While the footing settlements are small at low base excitations, they increase very rapidly at higher excitations. One of the main components of settlement is due to a softening of the foundation soil.

1 INTRODUCTION

Structures resting on loose saturated cohesionless deposits are susceptible to significant damage, if not complete failure, during strong earthquakes. Such failures are well documented in practically all major earthquake damage reports. The most common reason for the poor performance of footings resting on cohesionless material has been the loss of strength and stiffness of the foundation soil caused by the generation of residual porewater pressure.

It is generally agreed that the seismic performance of a structure can best be judged in terms of its deformation. The foundation displacements that can be tolerated depend upon the associated functional aspects of the structure being considered. These displacements are, in most cases, the result of deformation in the foundation soil. The deformations in loose saturated cohesionless soils can be divided into three basic components (Chang, 1984; Siddharthan, 1984): (1) a cyclic component associated with cyclic load, (2) a residual component due to a softening of the soil, and (3) additional deformation due to grain slip. Since the duration of the seismic excitation is short, only the first two components occur during shaking; the third component occurs afterward with dissipation of the induced porewater pressure.

Several laboratory investigations on the settlement of foundations have been reported in the literature. De Alba et al. (1976), Heller (1977), and Yoshimi and Tokimatsu (1977) have reported on the behavior of small footings subjected to base excitation on large shake tables. Recently, Whitman and Lambe (1982) and Finn et al. (1985) have reported the results of a series of centrifuge tests carried out at Cambridge University. In these tests, the porewater pressures, accelerations, and settlements of footings were generally measured. The associated study of the data has revealed these interesting features: a) a substantial part of the footing settlement is caused by a softening of the deposit; b) the porewater pressure ratios in the soil directly beneath the foundation are substantially less than the ratios in the soil at a distance from the foundation; c) during excitation, the foundation moves steadily downward with little or no intermittent upward movement; and d) at larger excitations, substantially higher settlements occur even though the porewater pressure ratios under the structure are small.

Since foundation settlement during excitation is primarily a function of the softening of the deposit, a method of analysis carried out in the time domain that accounts for the generation of residual porewater pressure is necessary. Furthermore, nonlinear hysteretic soil behavior should be accounted for. Chang

(1984), Siddharthan (1984), and Bouckovalas et al. (1986) have presented methods to compute the seismic displacement of foundations based on the effective stresses. The methods proposed by Chang (1984) and Bouckovalas et al. (1986) do not account for the structure's inertia effect upon the foundation response nor for other dynamic soil-structure interaction effects. While these factors may not be important under wave loading conditions, the effects of these factors for seismic loading conditions are important. On the other hand, the applicability of the method proposed by Siddharthan (1984) which does account for these factors has been verified to a limited extent by comparing computed residual porewater pressures and acceleration histories with centrifuge test results after Finn et al. (1984a,b).

In this paper, the capabilities of Siddharthan's two-dimensional effective stress analysis for predicting the response of the soil deposit and the footing resting on the surface of the deposit is described. First, the computed response is compared with available records of observed response from centrifuge tests. Thereafter, the influence of factors such as the location of the water table, the rocking of the foundation, the contact pressure, and the strength of the excitation on the response of the footings is reported.

2 PROPOSED METHOD OF ANALYSIS

In the dynamic analyses of soil-structure systems, it is often assumed that the loading imposed by seismic excitation can be superimposed on the long-term (static) equilibrium conditions. Since the dynamic soil properties, such as strength and stiffness, depend upon insitu stresses, the static stress condition should be evaluated first. The incremental elastic (tangent) approach which simulates layer construction (Duncan and Chang, 1970) can be used for this purpose. Thereafter, the incremental displacements between two time steps during the base excitation can be computed by solving the following set of dynamic incremental equilibrium equations.

$$[M]\{\Delta\ddot{x}\} + [C]\{\Delta\dot{x}\} + [K]_t\{\Delta x\} = -[M]\{I\}\Delta\ddot{U}_g(t) \qquad (1)$$

in which [M] is the diagonal mass matrix, [C] is the viscous damping matrix, $[K]_t$ is the tangent stiffness matrix, {I} is the unit vector, $\Delta\ddot{U}_g(t)$ is the increment in either the horizontal or the vertical base acceleration, and $\{\Delta x\}$, $\{\Delta\dot{x}\}$, and $\{\Delta\ddot{x}\}$ are the incremental displacements, velocities, and accelerations of the nodes relative to the base. Depending on whether an equation is written for the horizontal or the vertical direction, $\Delta\ddot{U}_g(t)$ is the increment in the corresponding base acceleration component. The stress-strain relationships used in the analysis are an extension of the relationships developed by Finn et al. (1977) for level ground conditions. Soil response is modeled by combining the effects of shear and normal stresses. In shear, the soil is treated as a nonlinear hysteretic material exhibiting Masing behavior during unloading and reloading. The initial or skeleton shear stress-strain relationship is assumed to be hyperbolic. Therefore, the tangent shear modulus in an element required in the formulation of the global tangent stiffness matrix depends upon the current shear strain, the state of the effective stress, and the previous strain history. To model a condition with no volume change during excitation, the tangent bulk modulus is assumed to be a large value. The tangent stiffness matrix needs to modified at every time step to reflect the current stress-strain state. Hysteretic damping is accounted for by a modification of the tangent stiffness matrix. A small amount of viscous damping may be included in the analysis to account for damping from any nonhysteretic source. The cyclic component of the displacement at any time is simply the algebraic sum of the incremental values.

In an effective stress response analysis, the seismically induced porewater pressures need to be assessed. The Martin-Finn-Seed (1975) porewater pressure model has been used for this purpose. However, this model has been modified to account for the presence of initial static shear stress. The initial static shear stress influences the liquefaction potential curve and the rate of generation of porewater pressure (Vaid et al., 1979; Chang, 1982). In this model, the incremental residual porewater pressures are evaluated by first computing the incremental plastic strain that occurs under drained conditions and then multiplying this by the rebound modulus. Other researchers have proposed similar approaches (Arulanandan et al., 1985; Bouckovalas et al., 1984). The porewater pressure model constants can be selected to match the rate of porewater pressure generation and the liquefaction potential curves.

There is a limit to the amount of porewater pressure that can develop in a soil element. This limit is easy to estimate in the case of triaxial or simple shear tests in the laboratory. This is because the ultimate state of stress has to be on the Mohr envelop and because the effective stress path followed by the sample is predictable (Chang, 1982) given the boundary conditions of the sample. However, in a two-dimensional analysis, the effective stress path followed by an element cannot be predicted beforehand; therefore, the maximum residual porewater pressure that develops cannot be assessed independent of the dynamic loading. However, one way of limiting the porewater pressure that might develop would be to allow generation only until the stress path touches the Mohr envelop. It will be seen later that this treatment leads to very low porewater pressures at locations under the footing as compared to the values observed in the centrifuge tests. Consequently, it was decided to permit porewater pressure generation to continue until the effective minor principal stress reached a certain value. Poulos et al. (1985) suggest that, for a given soil, this value is a function of the void ratio only. After initially touching the failure envelope, the stress path should travel down the failure envelope until the above criterion is satisfied. With movement down the Mohr envelope, the Mohr circle of stress decreases in size. Accordingly, correction forces are applied in the finite element program to cause such a reduction in the affected elements.

To determine the stress path followed by an element, one needs to compute the state of the effective stresses during the dynamic loading. The method employed to do this is discussed below.

The incremental nodal equilibrium equations, with a consideration for the porewater pressure in the elements, can be expressed (Christian et al., 1970) as

$$\{\Delta P\} = [K]_t\{\Delta\delta\} + [K^*]\{\Delta U\} \tag{2}$$

in which $\{\Delta P\}$ is the incremental load vector, $\{\Delta\delta\}$ represents the incremental nodal displacements, $[K^*]$ is the porewater pressure stiffness matrix, and $\{\Delta U\}$ represents the element porewater pressures. This equation is used to compute the current effective stresses and deformations of the deposit due to the increase in porewater pressure. In other words, $\{\Delta\delta\}$ represents the displacements due to the softening of the deposit. Note that, in solving Eq. 2, $\{\Delta P\} = 0$ while the values of $\{\Delta U\}$ are computed based on the porewater pressure generation model. This part of the analysis is considered to be an extension of the initial static analysis; and, thus, stress dependent tangent shear and bulk modulus values are used in the computations. The effective stresses so calculated are then used to update soil property values that depend upon the effective stress.

When a dry sand sample is subjected to cyclic loading, plastic volume change, E_{vp}, occurs due to interparticle slip. The occurrence of E_{vp} is the reason for the porewater pressure generation in saturated sands under undrained cyclic loading conditions. When this porewater pressure is allowed to drain, a volumetric strain equal to E_{vp} occurs in the sample resulting in settlement. A number of researchers have studied this problem of settlement due to E_{vp} both in dry and saturated sandy deposits (Silver et al., 1971; Lee et al., 1974; Pyke et al., 1975). They concluded that the plastic volume change depends upon the amplitude of cyclic shear strain and the previous loading history, while it is independent of vertical stress.

During seismic excitation, the effective stresses decrease due to generated porewater pressures; and then, after the excitation, the effective stresses increase as porewater pressures dissipate. In principle, accounting for E_{vp} is possible by an appropriate selection of soil properties during this unloading-reloading process. However, the selection of appropriate soil properties leads to more uncertainties. Accordingly, the following approximate procedure is employed: 1) nonlinear stress dependent elastic bulk modulus values are used during the loading and unloading process and 2) then independently computed values of E_{vp} are used to assess deformations due to grain slip after porewater pressure dissipation is complete. The later computations are undertaken by treating E_{vp} in the same way that temperature induced strains are analyzed in structural mechanics.

Slip or contact elements have been incorporated into the analysis to represent the interface characteristics between the soil and the structural elements. The properties of the slip elements were assumed to be elastic and perfectly plastic with failure at the interface given by Mohr-Coulomb failure criterion.

3 APPLICATION OF THE METHOD OF ANALYSIS

The validation of the above proposed technique requires good prototype data with which to compare. While shaking table tests may predict foundation response in a phenomenological sense, they are not good for comparative studies because the behavior of soils under very low confining pressures is generally quite different from soil behavior under higher insitu pressures. However, with centrifuge model testing, one can obtain a similarity between model and insitu or prototype stresses by appropriately increasing centrifugal acceleration. This is particularly important relative to soils that exhibit stress dependent stress-strain properties. Modeling laws are then used to assess the prototype response based on model behavior. The principles of such centrifugal modeling are presented elsewhere by Schofield (1981).

3.1 Centrifuge tests

Whitman and Lambe (1982) reported a series of seismic tests on centrifuged models in which the centrifugal acceleration was about 80 g. Fig. 1 shows the model used in these tests. A uniform deposit of Leighton-Buzzard #120/200 sand of an average relative density of 56% supported a circular solid brass footing (with the footing representing a structure). The thickness of the deposit was 151 mm, and the diameter of the footing was 113 mm. The corresponding prototype deposit was 12.1 m in height, and the footing was 9.0 m in diameter. The average bearing stress beneath the footing under prototype conditions was 130 kN/m^2. The base excitation was generated by allowing the wheels of the centrifuge container to travel on a track mounted on the wall of the centrifuge chamber. The deposit was instrumented to measure the settlement of the footing and the deposit and, also, the porewater pressure at a number of locations in the deposit. In the tests, the input excitation was intended to be (prototype scale) ten sinusoidal pulses with a constant period of 1.0 sec. However, the actual input motion was somewhat different due to resonances and mechanical linkage clearances interfering with the motion of the centrifuge chamber especially during the initiation of the base motion. In the first series of tests, the water table was located very close to the surface at 0.5 m; and, in the other, it was located at 1.3 m below the foundation. A number of interesting observations were reported by Whitman and Lambe. For the case when the peak acceleration was 0.17 g, they found that, at points away from the footing, the porewater pressure rose quickly to become equal to the total vertical overburden pressure stress. However, lower porewater pressures were recorded below the footing. Furthermore, during the excitation, the footing settled progressively resulting in as much as 30 cm displacement with little or no tipping. After the cessation of the base motion, the porewater pressure, at points just under the footing, increased indicating a flow of porefluid toward the footing.

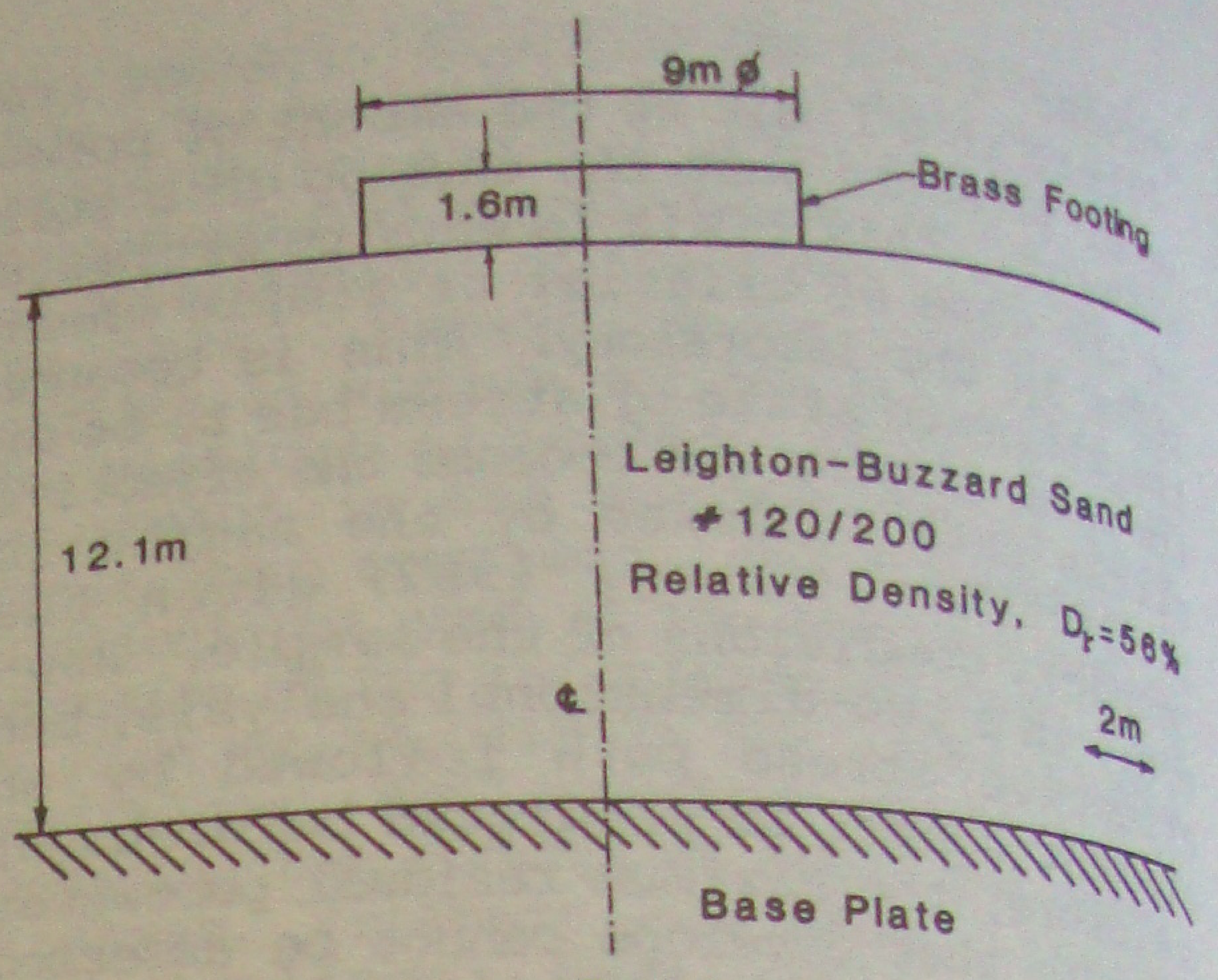

Fig. 1 Brass footing resting on sand (after Whitman and Lambe, 1982)

Since the recorded base excitation was not available, it was not possible to compare the computed and recorded responses on a point by point basis. Therefore, it was only possible to compare results phenomenologically. Details of the comparative study are presented subsequently.

3.2 Seismic response of surface footings

In order to investigate the importance of such factors as the contact pressure, the rocking of the structure, the location of the water table, and the strength of excitation on the behavior of footings, the response of the structure shown in Fig. 1 was evaluated for a variety of conditions. Since the engineering properties of #120/200 Leighton Buzzard sand at a relative density, D_r, of 56% are not readily available, the properties of Ottawa sand (C-109) were used in their

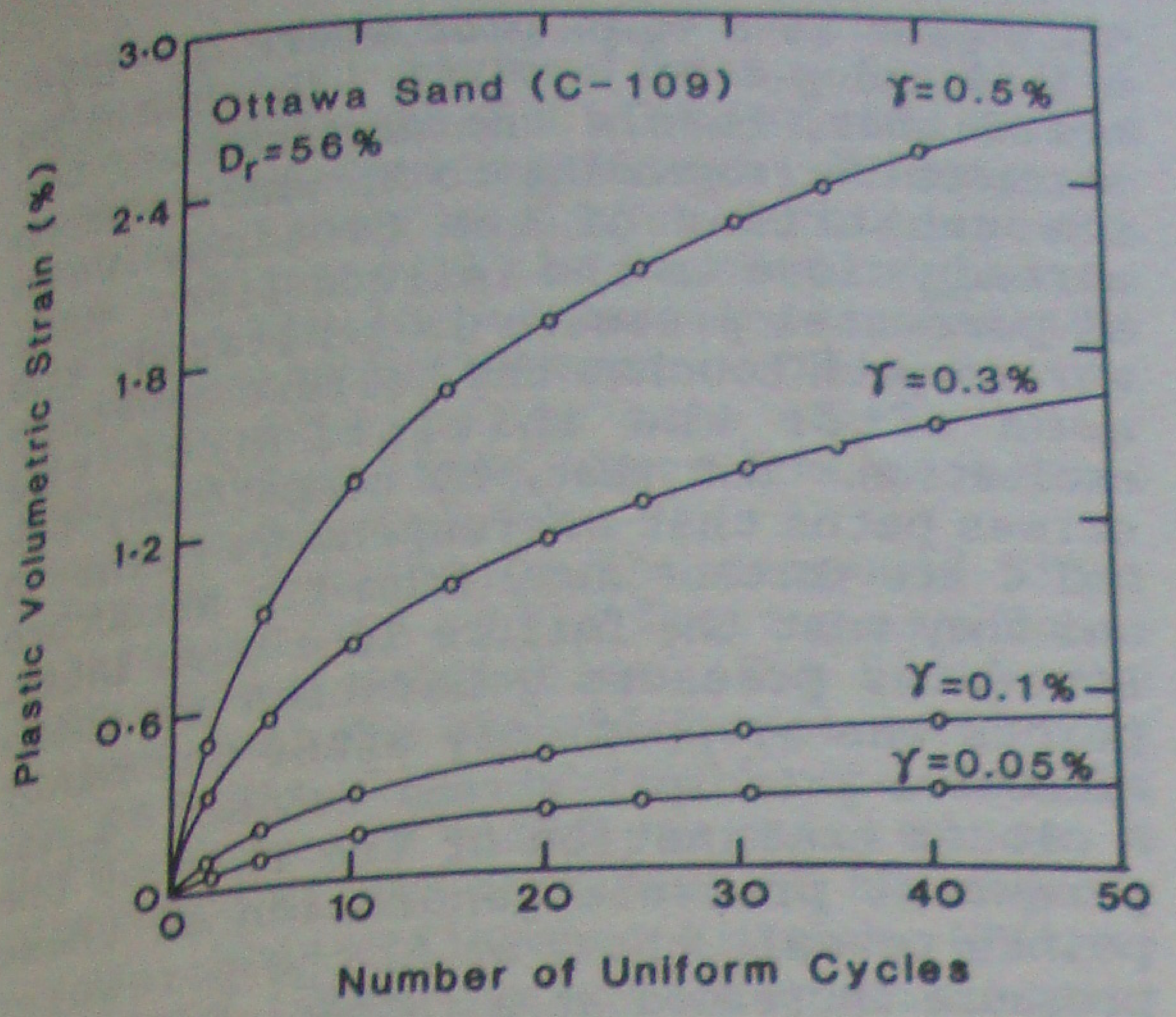

Fig. 2 Volumetric strain behavior

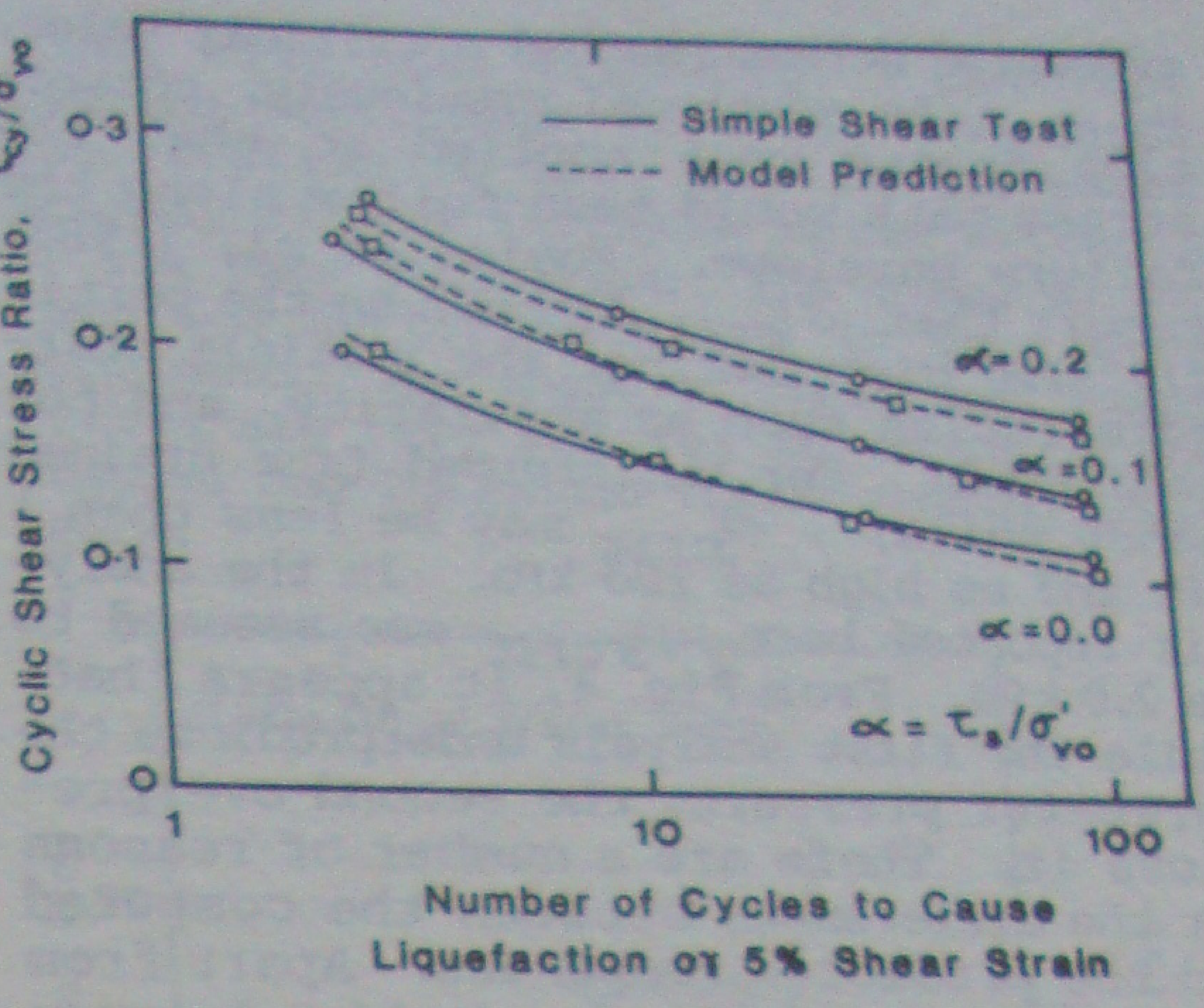

Fig. 3 Liquefaction potential curves

place in the response evaluation. Extensive laboratory studies on the cyclic behavior of Ottawa sand (C-109) have been reported in the literature by Bhatia (1980) and Vaid and Finn (1979). The porewater pressure generation model used in the analysis requires that the plastic volume change behavior of the dry sand at the given relative density be known. From the data on simple shear tests on Ottawa Sand provided by Bhatia (1980), the volume change characteristics of Ottawa sand at a relative density of D_r = 56% as a function of shear strain amplitude and the number of cycles were constructed as shown in Fig. 2. These curves were then used in the computation of the plastic volume change.

In addition, the porewater pressure generation model requires an evaluation of the rebound modulus of the sand. The parameters (which are a function of the initial static shear stress) used to evaluate the rebound modulus were selected so that the model was able to reproduce the rate of the porewater pressure generation and also the liquefaction potential curves. Data on porewater pressure generation in Ottawa sand at various relative densities as a function of the initial static shear stresses has been reported by Vaid and Finn (1979). The interpolated laboratory liquefaction curves that are relevant for D_r = 56% and the curves predicted by the porewater pressure generation model are shown in Fig. 3.

Figure 4 shows the variation in the maximum porewater pressure ratio (u/σ'_{vo}) which is the ratio of the maximum residual porewater pressure to the initial vertical effective stress along the centerline of the footing. A uniform sinusoidal base excitation of ten cycles with a period of 1.0 sec. was used in the response study. Porewater pressure ratios which were reported by Whitman and Lambe (1982) for a maximum input acceleration (a_{max}) of 0.17g are also given in the figure. Two analyses were performed as part of the present study. In the first, the porewater pressure generation was stopped as soon as the effective stress path touched the Mohr-Coulomb envelope. In the other, the porewater pressure generation was allowed to continue until the minor

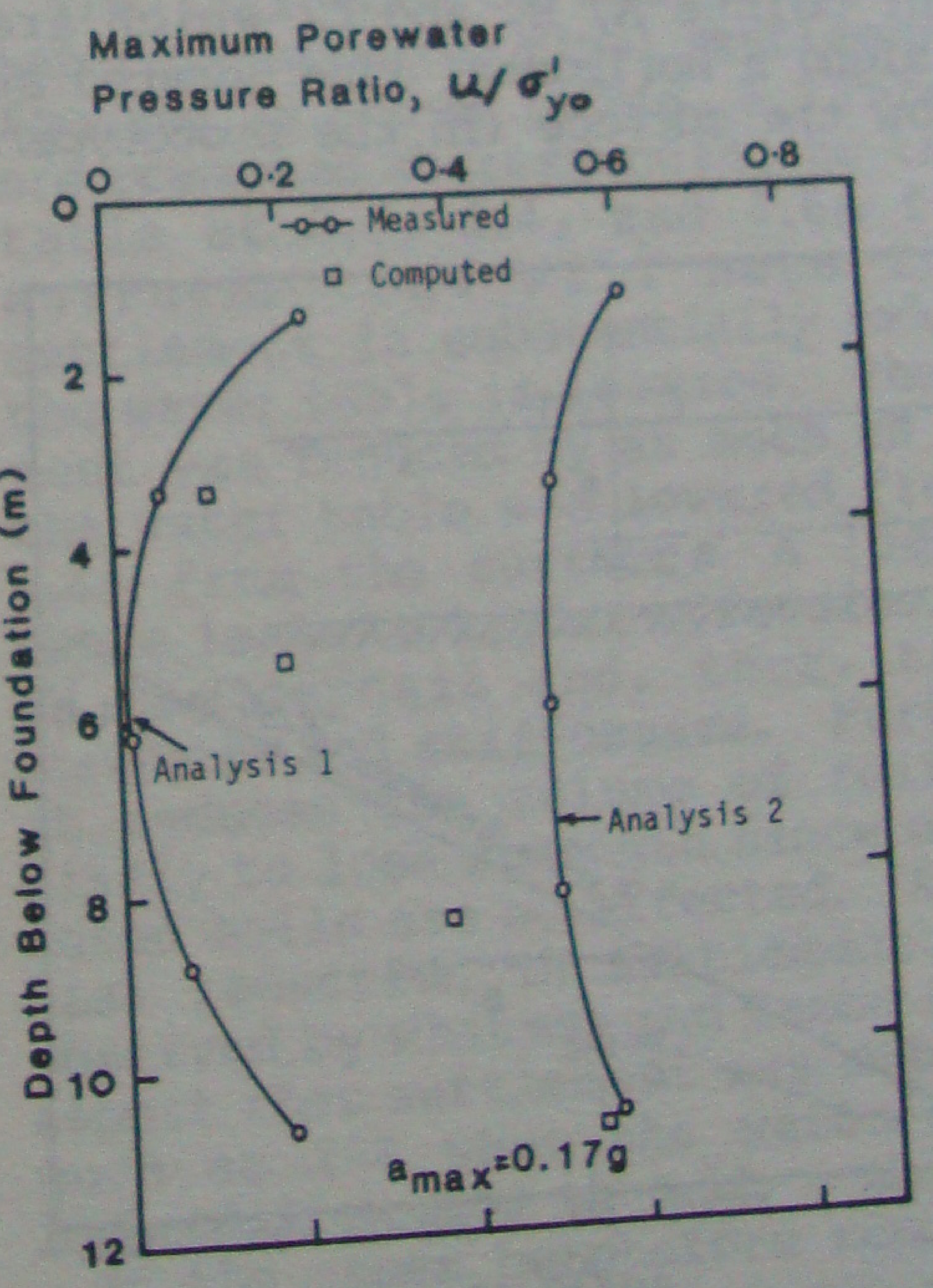

Fig. 4 Distribution of residual porewater pressure ratio

effective stress reached a critical value, σ'_{3crit}. As mentioned previously, correction forces were applied so that the stress path would then follow along the failure envelope. Poulos et al. (1985) report that σ'_{3crit} depends on the particle size distribution, the particle characteristics such as angularity, and the void ratio. For undisturbed fine grained sandy soils, σ'_{3crit} may be less than 1 kPa and as high as 100 kPa. In the analysis reported here, σ'_{3crit} was assumed to be 2.0 kPa. From Fig. 4, it appears that, while the first analysis underpredicts the porewater pressure, the second overpredicts it. There are a number of reasons for the differences between the computed and the predicted responses. Apart from the fact that the base excitation between the two are different, plane strain conditions were assumed in the computations which is different from the axisymmetry condition that exists in the model and prototype. Secondly, since σ'_{3crit} is a function of overburden pressure (or void ratio), it should vary from point to point. It was decided not to adjust σ'_{3crit} because of uncertainties in its selection. It should be noted that, while the porewater pressures predicted under the footing by the aforementioned two methods differed from the observed values, the predictions at points away from the footing matched the recorded values. This can be better explained by considering the stress paths of a number of points.

Figure 5 shows the effective stress paths for points A, B, and C, which are located along a horizontal line located at 8.4m below the surface (in the prototype).

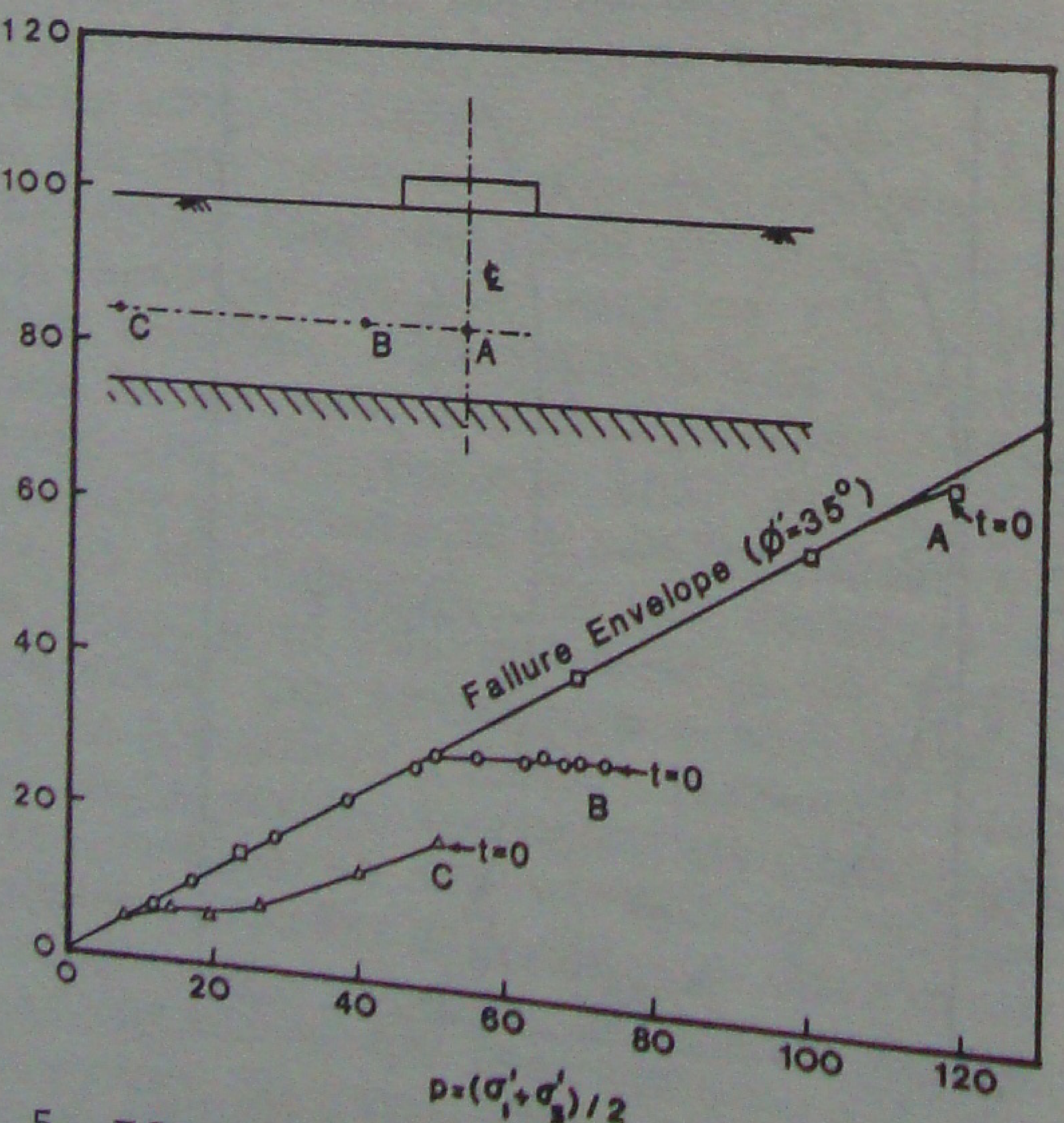

Fig. 5 Effective stress paths of elements

This plot is a (q,p) plot where $q = (\sigma'_1 - \sigma'_3)/2$ and $p = (\sigma'_1 + \sigma'_3)/2$. It should be noted that, before the earthquake, the stresses corresponding to A, which was on the centerline of the footing, were already close to the failure line. And, as porewater pressure is generated, the stress path touches the failure envelope soon after the initiation of the excitation. Not that, by comparison, the stress paths that correspond to points B and C are further away from the structure and they meet the failure line much later. Porewater pressure generation at these points was stopped only after the minor effective principal stress reached σ'_{3crit}. A closer examination of the rate of the porewater pressure generation at these points reveals that, at A, the porewater pressure increased at a faster rate and it stabilized within two seconds after the initiation of excitation. However, at C - far from the structure (i.e., in the free field) - the porewater pressure increased at a slower rate and stabilized when it approached the initial overburden pressure. This phenomenon was also observed in the results reported by Whitman and Lambe (1982).

As pointed out earlier, the displacement during excitation has two parts: a cyclic component (δ_{cy}) and a component due to a softening of the soil (δ_{so}). The computed value of the total settlement, $\delta_t (= \delta_{cy} + \delta_{so})$, and the component δ_{so} at the corner of the footing for the excitation with a_{max} = 0.17g are shown in Fig. 6. The difference between the two computed curves is the cyclic component, δ_{cy}. It should be noted that the footing response was computed for two seconds beyond the cessation of the shaking. One will also note that, because nonlinear hysteretic material properties were used, the cyclic component of deformation, δ_{cy}, did not return to zero at the cessation of the

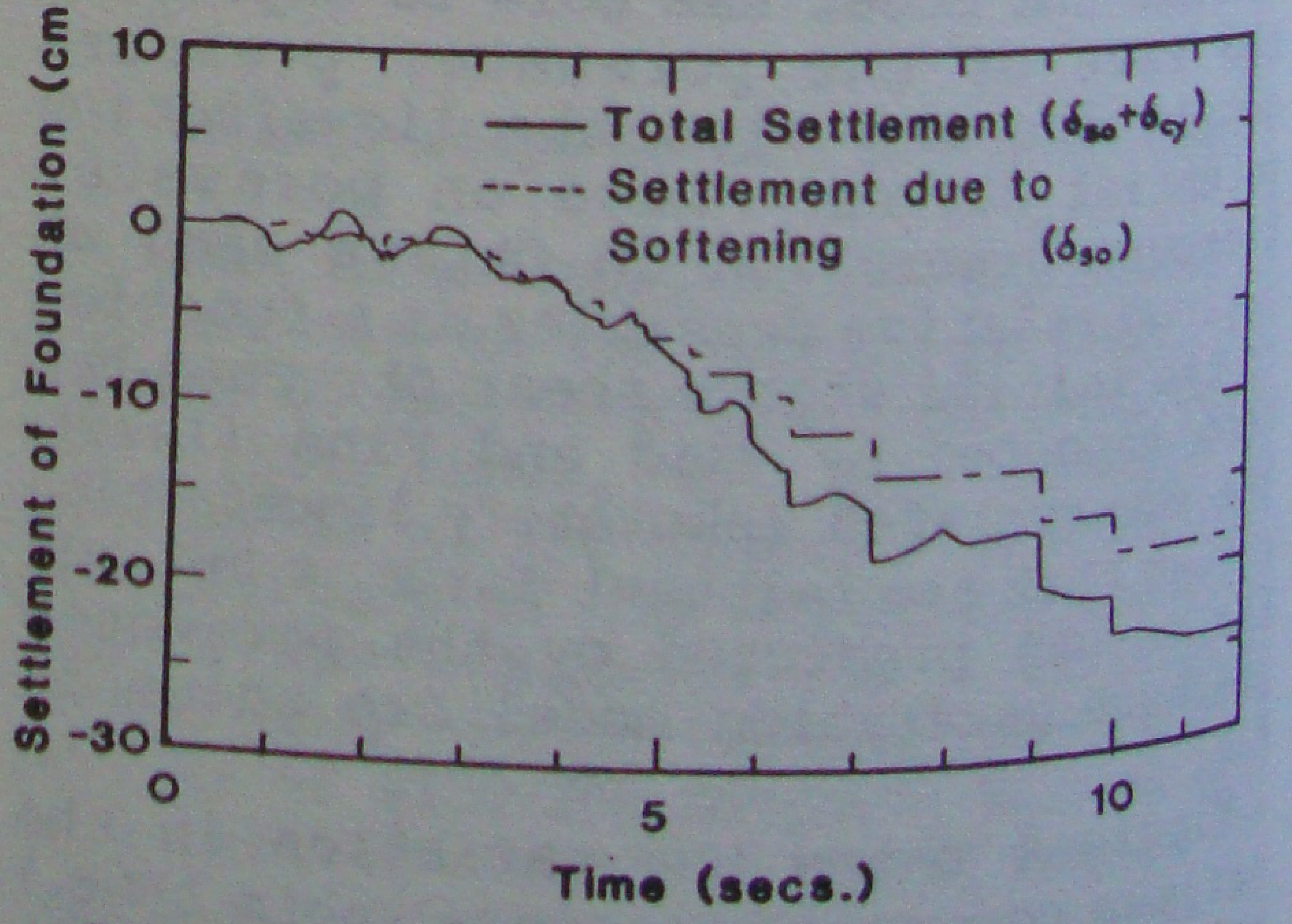

Fig. 6 Settlement of footing during excitation

shaking. Initially, the settlement remained small (up to 4 secs. of shaking) after which the settlement increased rapidly and then stabilized. Finally, it is clear from Fig. 6 that settlement due to a softening of the deposit, δ_{so}, constitutes the larger part (more than 80%) of the total settlement. (This was not strictly true in the case of the lower base accelerations where low porewater pressures developed.)

Figure 7 presents the computed final settlement (ρ_f) of the footing as a function of base excitation. The final settlement includes the additional settlement due to grain slip. One will note that the settlement is also presented as a percentage of the thickness of the deposit (ρ_f/D). The settlements given by Whitman and Lambe (1982) are relative settlements evaluated with respect to the surrounding soil. Therefore, computed and recorded relative settlements are also shown in the figure. Even though Whitman and Lambe have presented a substantial amount of centrifuge test data, only three test results were used in Fig. 7. This is because the centrifuge tests at Cambridge University were carried out consecutively on a single model going from a lower base acceleration to a higher one. In this type of test procedure, the sand progressively densifies and, thus, the properties differ from those of the original soil. Therefore, only the test results that correspond to a first excitation were plotted.

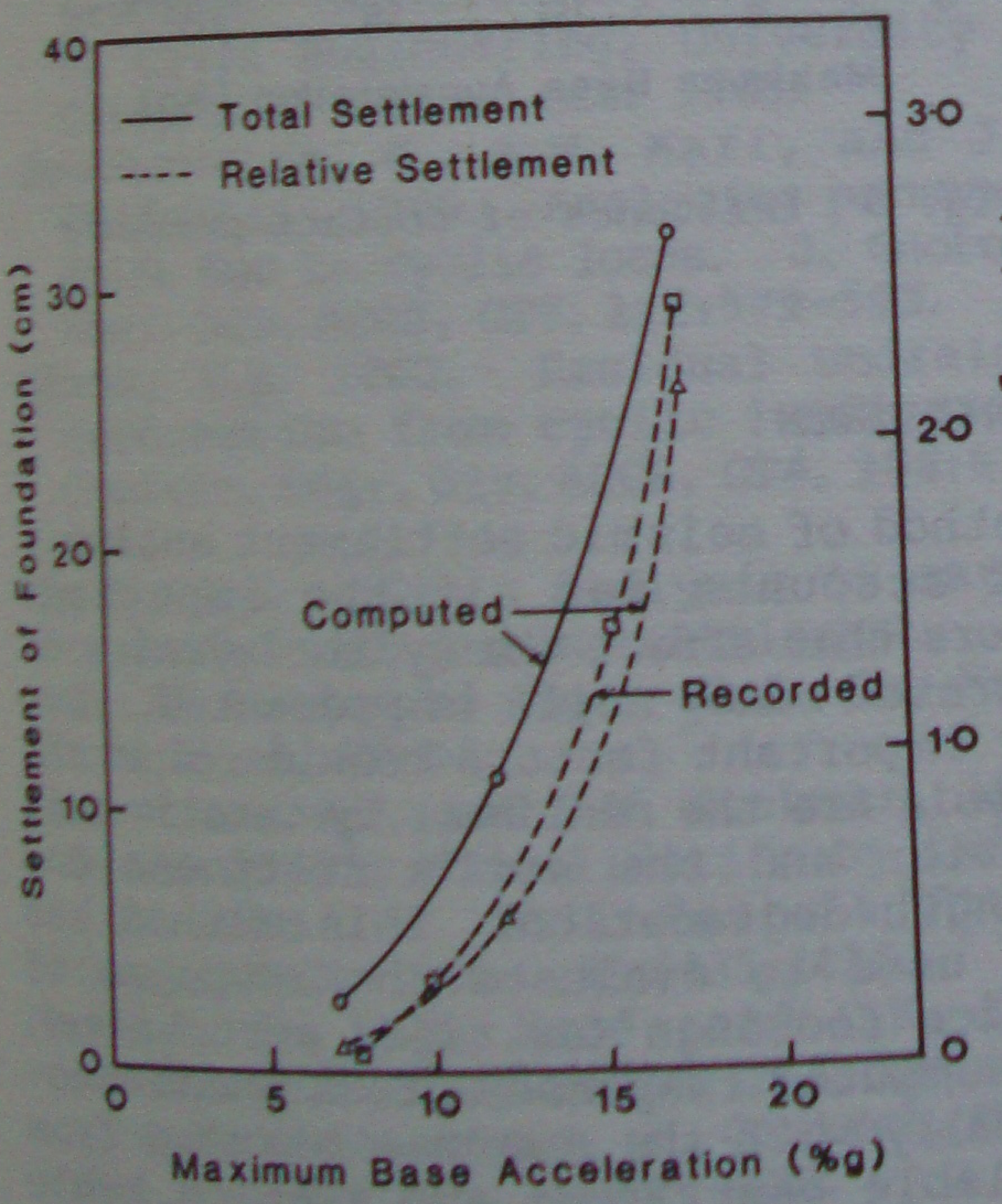

Fig. 7 Final settlement of footing

One will note from Fig. 7 that the footing settlement is small when base acceleration is low, but it increases rapidly with an increase in the strength of the base excitation. The computed and recorded settlements are in very good agreement. The shape of these settlement curves are very similar to those of the Yoshimi and Tokimatsu (1977) shaking table tests.

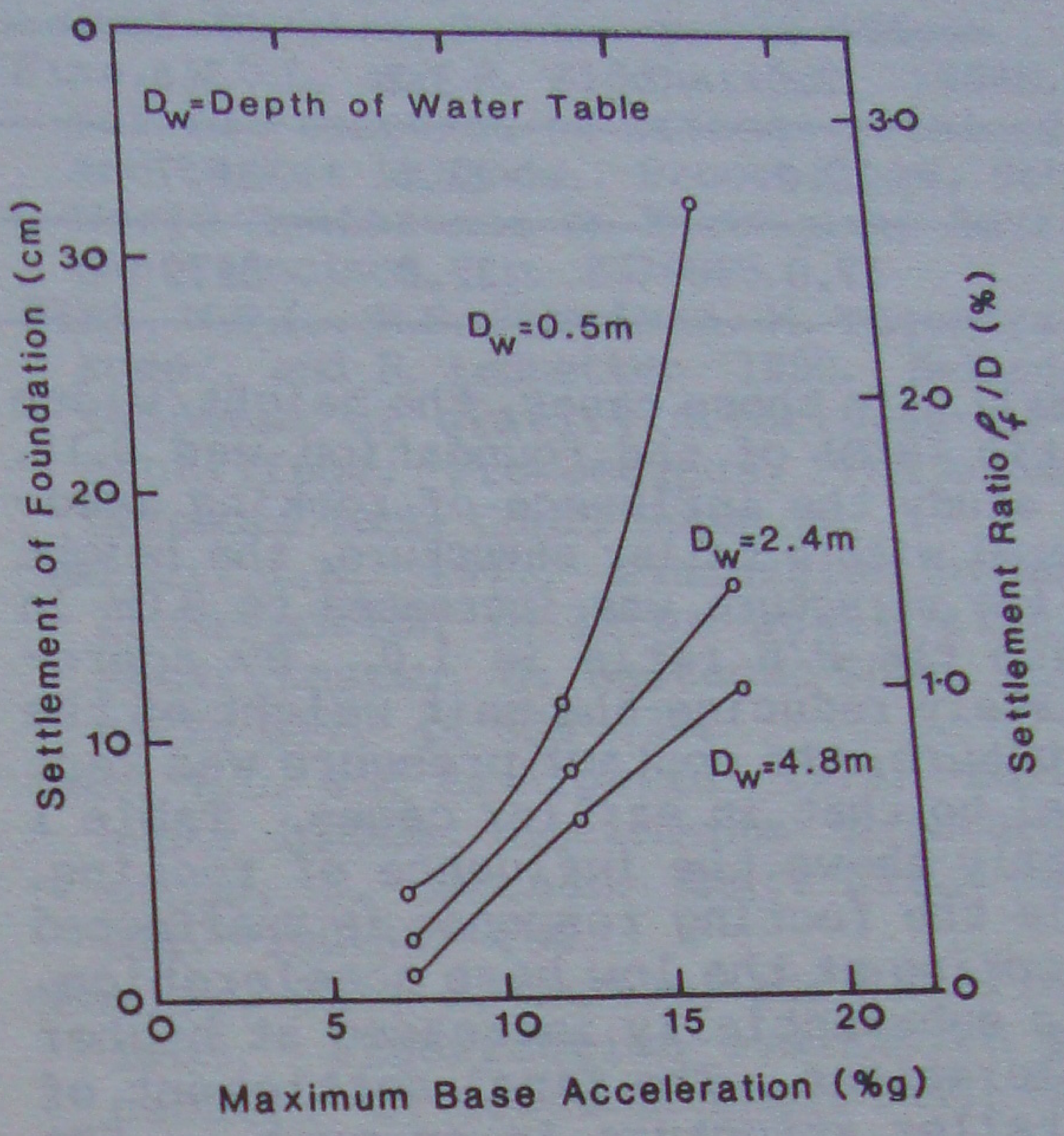

Fig. 8 Influence of the location of water table

The influence of the location of the water table on the final settlement of the footing is shown in Fig. 8. Three cases are presented corresponding to the water table at 0.5, 2.4, and 4.8m from the surface. One will note that the settlement is substantially reduced when the water table is lowered. The settlement was reduced by as much as 50% when the water table was lowered from 0.5 to 2.4m from the surface. A lower water table leads to higher effective stresses in the deposit and, thus, to higher strengths and stiffnesses. Furthermore, it reduces the volume of soil that is likely to lose strength since only saturated soils are so affected. A substantial reduction in settlement was also observed by Whitman and Lambe (1982) who report that settlement was reduced by as much as 25% when the water table was lowered from 0.5m to 1.3m.

In the cases heretofore reported, the height of the structure was only 1.6m; and, therefore, the influence of foundation rocking upon the overall response was

TABLE 1

Maximum Input Acceleration %g	Final Settlement of the Foundation (cm) H/B 0.18	1.0	Maximum Horizontal Displacement of the Foundation (cm) H/B 0.18	1.0	Maximum Horizontal Acceleration of the Foundation %g H/B 0.18	1.0
7.0	3.2	3.6	2.5	2.0	11.2	12.0
12.0	11.5	16.7	25.2	20.6	16.2	24.9
17.0	32.8	54.9	31.8	34.1	20.4	22.4

small. In those cases, the height/width ratio (H/B) of the foundation was 0.18. To study the influence of rocking associated with a taller structure, the height of the structure was increased to 9.0m in which the H/B ratio is 1.0. By appropriately reducing the unit weight of the structure, the contact pressure was kept equal to that in earlier cases. Table 1 clearly shows the influence of rocking. While the footing response is unaffected by rocking at the low base acceleration, it is substantially increased at higher accelerations. The final settlement of the taller structure is as much as 67% larger than that of the shorter structure. It appears that the influence of rocking is substantial and, therefore, needs to be addressed in response studies.

The influence of contact pressure on the final settlement of the footing is depicted in Fig. 9. In the cases considered, the height of the structure is again 1.6m. The contact pressure is increased from $0.5q_o$ to $1.5q_o$ by appropriately increasing the unit weight of the footing. Here $q_o = 130\ kN/m^2$. As expected, an increase in contact pressure can substantially affect the settlement of the footing but only at higher accelerations. At low base excitation, there is little effect. This is because the settlement caused by the softening of the deposit was minimal at low base excitation. However, at higher base excitation, the higher contact pressure leads to a substantial increase in the settlement component due to a softening of the deposit. A similar variation in foundation settlement was observed in the shaking table tests performed by Yoshimi and Tokimatsu (1977).

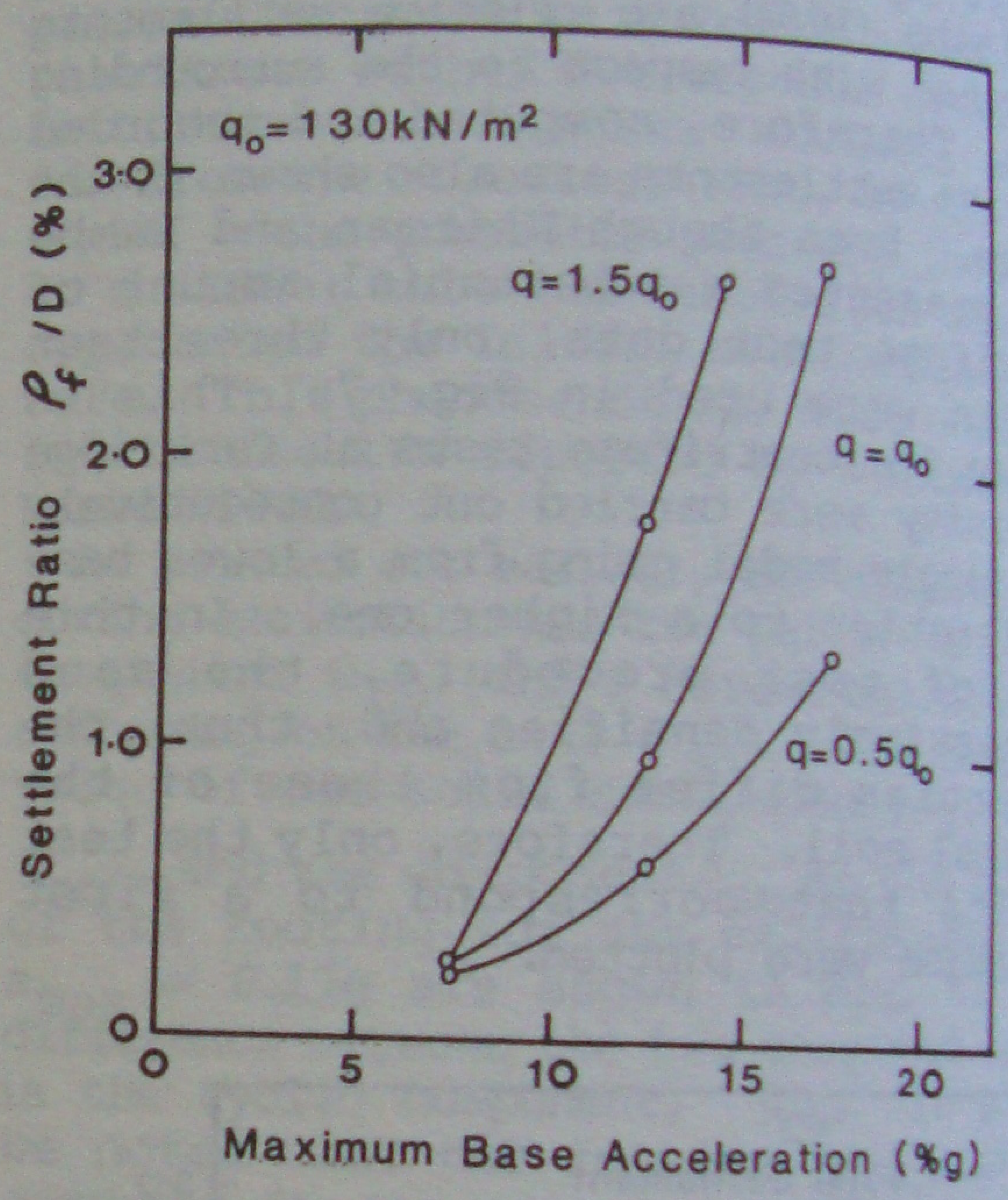

Fig. 9 Influence of contact pressure

4 CONCLUSION

A method of seismic settlement analysis that accounts for all the important factors that affect the cyclic behavior of saturated sandy soils is presented. Two very important factors considered in the analysis are the nonlinear hysteretic soil behavior and the soil's stiffness and strength degradation. This method has been used to evaluate the response of surface footings (or rigid structures). The computed response agrees phenomenologically with the response reported from available centrifuge and shaking table tests.

A parametric study relative to a fine uniform medium dense sand deposit 12.1 meters thick supporting a rigid footing has been reported. This study reveals that it is important to keep track of the effective stress paths followed by the different soil elements and, secondly, that porewater pressures seem to increase even after the path has intersected the Mohr failure envelope. The parametric study confirms that factors such as a rocking of the structure, the location of the water table, contact pressure, and the strength of the base excitation have a significant influence on the settlement response. For example, settlement was reduced by as much as 50% when the water table was lowered from 0.5 to 2.4m below the surface; and, at low levels of base excitation, the footing settlements were low, but they increased very rapidly as the strength of the excitation increased.

5 ACKNOWLEDGEMENTS

Special thanks are due to Jeanie Pratt for her excellent typing. This study was funded by an Engineering Research Initiation Grant from the Engineering Foundation. Their support is gratefully acknowledged.

6 REFERENCES

Arulanandan, K. and K. Muraleetharan. Soil liquefaction - a boundary value problem. Research Report, Department of Civil Engineering, University of California, Davis. Oct. 1985.

Bouckovalas, G., A.W. Marr, and J.T. Christian 1986. Analyzing permanent drift due to cyclic loads. J. Geotech. Engr. Div. ASCE, GT6. 112:579-593.

Chang, C.S. 1982. Residual undrained deformation from cyclic loading. J. Geotech. Engr. Div. ASCE, GT4. 108:637-646.

Chang, C.S. 1984. Analysis of earthquake induced footing settlement. 8th World Earthquake Engr. Conf. San Francisco. p. 87-94.

Christian, J.T. and J.W. Boehmer 1970. Plane strain consolidation by finite elements. J. Soil Mech. & Found. Engr., ASCE, SM4. 96:1435-1455.

DeAlba, P., H.B. Seed, and C.K. Chan 1976. Sand liquefaction in large scale simple shear tests. J. Geotech. Engr. Div., ASCE, GT9. p. 909-928.

Duncan, J.M. and C.Y. Chang 1970. Nonlinear analysis of stress and strain in soils. J. Soil Mech. & Found. Div., ASCE, SM5, 96:1629-1653.

Finn, W.D.L., K.W. Lee, and G.R. Martin 1977. An effective stress model for liquefaction. J. Geotech. Engr. Div., ASCE, GT6, 103:517-533.

Finn, W.D.L., R. Siddharthan, F. Lee, and A.N. Schofield 1984a. Seismic response of drilling islands in a centrifuge including soil-structure interaction. Proceedings, 16th Annual Offshore Tech. Conf. Houston, Texas. p. 399-406.

Finn, W.D.L. and R. Siddharthan 1984b. Seismic response of caisson-retained and tanker islands. Proceedings, 8th World Conference on Earthquake Engr. San Francisco. p. 857-865.

Finn, W.D.L., R.S. Steedman, M. Yogendrakumar, and R. Ledbetter 1985. Seismic response of gravity structures in a centrifuge. Proceedings, 17th Annual Offshore Tech. Conf. Houston.

Heller, L.W. 1977. Discussion on sand liquefaction in large-scale single shear tests. J. Geotech. Engr. Div., ASCE, GT7. p. 834-836.

Lee, K.L. and A. Albaisa 1974. Earthquake induced settlements in saturated sands, J. Geotech. Engr. Div., ASCE, GT4. 100:387-406.

Poulos, S.J., G. Castro, and J.W. France 1985. Liquefaction evaluation procedure. J. Geotech. Engr. Div., ASCE, #6. 111:772-792.

Pyke, R., H.B. Seed, and C.K. Chan 1975. Settlement of sands under multi-directional shaking. J. Geotech. Engr. Div., ASCE, GT4, 101:379-398.

Siddharthan, R. 1984. A two-dimensional nonlinear static and dynamic response analysis of soil structures. Thesis submitted in partial fulfillment of the requirements for a Ph.D., Univ. of British Columbia, Vancouver, Canada.

Silver, M.L. and H.B. Seed 1971. Volume change in sands during cyclic loading. J. Soil Mech. & Found. Engr. Div., ASCE, SM9, 97:1171-1182.

Vaid, Y.P. and W.D.L. Finn 1979. Effect of static shear on liquefaction potential. J. Geotech. Engr. Div., ASCE, GT10. 105:1233-1246.

Whitman, R.V. and P.C. Lambe 1982. Liquefaction: consequences for a structure. Proceedings of Conf. on Soil Dyn. & Earthquake Engr., Southampton. p. 941-949.

Yoshimi, Y. and K. Tokimatsu 1977. Settlement of buildings on saturated sand during earthquakes. Soils and Found., #1. 17:23-38.